water

MDPI

Article

Towards i5 Ecohydraulics: Field Determination of Manning's Roughness Coefficient, Drag Force, and Macroinvertebrate Habitat Suitability for Various Stream Vegetation Types

Christos Theodoropoulos [1,*], Georgios Vagenas [1,2], Ioanna Katsogiannou [2], Konstantinos Gritzalis [2] and Anastasios Stamou [1]

[1] Department of Water Resources and Environmental Engineering, National Technical University of Athens, 5 Iroon Polytechniou Str., 15780 Athens, Greece
[2] Institute of Marine Biological Resources and Inland Waters, Hellenic Centre for Marine Research, 46.7 km Athens-Sounio Ave., 19013 Anavyssos, Greece
* Correspondence: thchristo@sch.gr; Tel.: +30-22910-76395

Abstract: Ecohydraulic models have commonly used the flow velocity, water depth, and substrate type (i3 models) as the three fundamental determinants of the distribution of freshwater biota, but a fourth determinant has largely been neglected: stream vegetation. In this study, we provide the hydraulic and habitat information required to develop vegetation-adapted ecohydraulic models (i4 models) in streams. We calculated drag forces and Manning's roughness coefficients (n_V) for nine types of submerged, emergent, and overhanging stream vegetation. In addition, we developed habitat suitability curves (HSCs) for benthic macroinvertebrates for these stream vegetation types. Hydraulic modules can now be upgraded to simulate stream vegetation by including the vegetation-adapted n_V values within an additive approach in which n_V is added to the n value of the inorganic substrate to which the vegetation is rooted. Habitat modules can also be upgraded to include macroinvertebrate HSCs for stream vegetation, again by adding the vegetation-adapted habitat suitability to that of the inorganic substrate to which the vegetation is rooted. In combination, i4 ecohydraulic models (including vegetation) can now be designed and applied, and we suggest that ecohydraulic research should further focus on including a fifth variable (water temperature) to ultimately advance to i5 ecohydraulic models that will optimally simulate the hydroecological reality.

Keywords: hydroecological models; ecohydrology; hydrodynamic habitat models; vegetation models; habitat preferences

Citation: Theodoropoulos, C.; Vagenas, G.; Katsogiannou, I.; Gritzalis, K.; Stamou, A. Towards i5 Ecohydraulics: Field Determination of Manning's Roughness Coefficient, Drag Force, and Macroinvertebrate Habitat Suitability for Various Stream Vegetation Types. *Water* **2022**, *14*, 3727. https://doi.org/10.3390/w14223727

Academic Editors: Giuseppe Francesco Cesare Lama and Gianluigi Busico

Received: 20 October 2022
Accepted: 15 November 2022
Published: 17 November 2022

1. Introduction

It has been more than 60 years since the development of the first computational fluid dynamics (CFD) model in the Los Alamos National Laboratory (1957; Los Alamos, NM, USA; [1]), which could solve the equations of fluid motion to simulate flow dynamics. Since then, CFD models have been routinely coupled with ecological/habitat models (and termed 'ecohydraulic models') to facilitate the management of freshwater ecosystems by, e.g., assessing the environmental flows downstream of dams [2,3], evaluating the ecological effectiveness of river restoration [4,5], or ecologically optimizing fish passage through fishways [6,7].

Ecohydraulic models have been founded on a long-proven theory that physical (hydraulic) variables (mainly flow velocity (V), water depth (D), and substrate type (S)) are major determinants of the distribution of freshwater biota [8,9]. Regardless of purpose, these models commonly include the following processes: A hydraulic model (CFD-based) calculates V and D in various water discharges across a computational mesh simulating a river reach by solving the equations of fluid motion (conservation of mass and x-wise, y-wise, and z-wise momentum, depending on the spatial resolution required). Then, a

coupled habitat model combines the calculated V and D at each node of the mesh with S and compares all V-D-S combinations (node by node) with the a priori known V-D-S preferences of selected freshwater biota (mainly fish, benthic macroinvertebrates, and aquatic plants) to simulate/predict their instream distribution or to calculate the suitability of each V-D-S combination in the river reach in the various simulated discharges [10,11]. However, despite the progress that has been made, a fourth fundamental determinant of the distribution of freshwater biota has been neglected by most ecohydraulic simulations: stream vegetation [12,13].

Stream vegetation (i.e., vegetation on the bottom of a river or riparian vegetation that falls into the water) shapes freshwater communities either directly, by providing additional instream habitats for freshwater biota, thus increasing habitat and biological diversity [14,15], or indirectly, by altering local hydraulics (increasing flow resistance, mostly leading to slower and deeper waters [15,16]). Consequently, ecohydraulic models not accounting for the hydroecological influence of stream vegetation may produce less robust environmental flow recommendations [17] or less confident results on the effectiveness of river restoration [18–20]. To account for stream vegetation, ecohydraulic models require specific adjustments in both their hydraulic and ecological/habitat modules.

Hydraulic models/modules consider stream vegetation as a variable that increases water flow resistance [18,21], and thus hydraulic research has focused on calculating the appropriate roughness coefficients to account for vegetation-induced hydraulic effects on the flow field [22–24]. To this end, stream vegetation has been commonly categorized into emergent and submerged, rigid and flexible. The flow field has been subdivided into layers, and simple or complex equations have been formulated to appropriately calculate vegetation-adapted bed roughness coefficients (Manning's hydraulic roughness coefficient (n) has been commonly used) or drag force terms for the above vegetation types [15,24–27], accounting for vegetation density, flexibility, submergence, shape, etc. [28,29]. However, despite the progress that has been made, hydraulic simulations in the presence of stream vegetation are associated with uncertainty regarding the accuracy of the hydrodynamic calculations [30] (similar to other types of hydraulic models, e.g., sea-based [31,32]) due to the lack of appropriate data for validation. Consequently, although there is a growing theoretical background for incorporating stream vegetation in hydraulic models, there is currently a lack of field data around real vegetation patches to enable the practical application of these equations in hydraulic (or ecohydraulic) models [33].

Habitat models/modules consider stream vegetation as another habitat-defining variable, along with V, D, and S. The preference of freshwater biota for V, D, and S is commonly calculated and visualized either with habitat suitability curves (HSCs) [34] or (fuzzy) habitat suitability rules [35,36] in which a zero value reflects a complete absence of aquatic organisms (totally unsuitable habitat) and a value of one represents the maximum presence (totally suitable habitat). However, although there are several V-, D-, and S-based suitability curves available worldwide (and thus, V-D-S-based ecohydraulic models can be easily formulated), as far as we are aware, there is a lack of vegetation-based HSCs, which, however, are a prerequisite to practically apply vegetation-adapted ecohydraulic models.

The purpose of this study was to provide the hydraulic and habitat information required to develop and apply vegetation-adapted ecohydraulic models in streams. Using hydraulic and biological field measurements from two stream reaches in Greece, we calculated drag forces and Manning's roughness coefficients for various types of submerged, emergent, and overhanging stream vegetation. We also developed HSCs for benthic macroinvertebrates for these stream vegetation types. Ecohydraulic scientists and practitioners can now use the calculated vegetation-adapted Manning's roughness coefficients to calibrate and validate a robust vegetation-including hydraulic module and can use the vegetation-based HSCs to properly include stream vegetation as a fourth habitat-defining variable, thus increasing the accuracy of the habitat module and ultimately producing ecohydraulic models that optimally simulate hydroecological reality.

2. Materials and Methods

2.1. Presampling

Prior to sampling, stream vegetation was categorized into nine types: (1) algae, (2) bryophytes, (3) emergent fine-leaved plants (EFL), (4) emergent broad-leaved plants (EBL), (5) submerged fine-leaved plants (SFL), (6) submerged broad-leaved plants (SBL), (7) overhanging (tree trunks, bush branches, and stems that fall from the river bank to the water surface), (8) free-floating vegetation (e.g., water lilies), and (9) detritus (snags, dead branches, leaves, and roots).

2.2. Sampling

We sampled 124 vegetated microhabitats (rectangular-shaped; 0.0625 m^2) of the above types from two stream reaches in the region of Attica, Greece: (i) the Oinoi Stream and (ii) the upper Great Rafina River (Lykorema Stream) (Figure 1). A total of 74 microhabitats were sampled in spring 2021 (high-flow period) and 50 microhabitats were sampled in summer 2021 (low-flow period) within a stratified sampling framework to evenly allocate vegetation types among the samples.

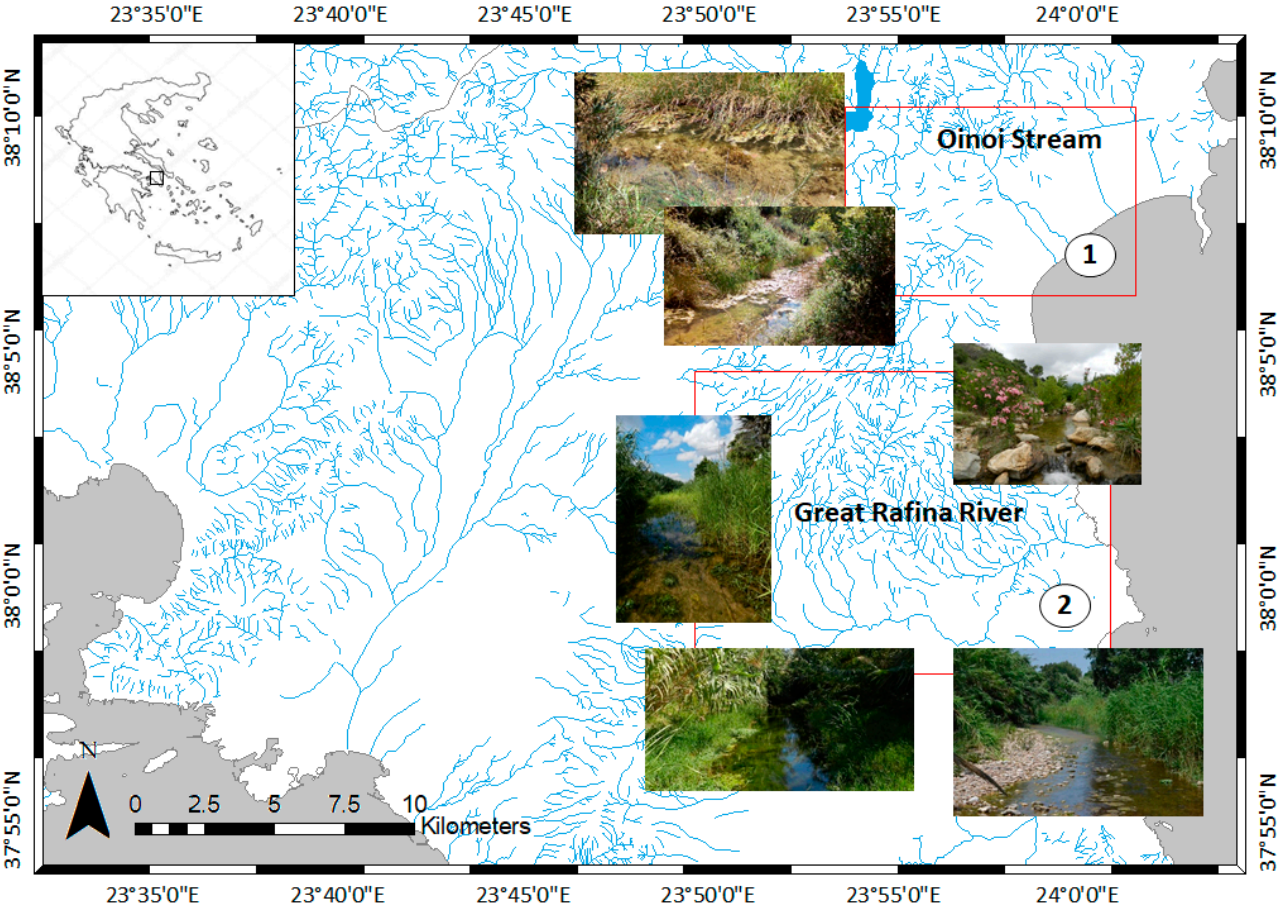

Figure 1. Study area. The Oinoi Stream and the upper Great Rafina River (Lykorema Stream), Attica, Greece, in which 124 vegetated microhabitats were sampled in spring and summer 2021.

At each microhabitat/sample, we (1) recorded the type and density (percent cover) of vegetation (visual estimation; photos were taken to further justify our selection), (2) measured the flow velocity and water depth before, after, and on each side of the microhabitat (using the Swoffer 2100 current velocity meter and a water depth measurement rod attached to the velocity meter), and (3) collected a sample of benthic macroinvertebrates (Figure 2). Macroinvertebrates were sampled using a 0.25 × 0.25 = 0.0625 m^2 Surber sampler (or a hand net of the same dimensions) with a 500 μm mesh size. Samples were preserved

in plastic bottles containing 70% ethanol. In the laboratory, all specimens were sorted and identified to the family level using a stereo microscope (magnification 6.39–639) and macroinvertebrate identification guides for the Mediterranean region [37–39].

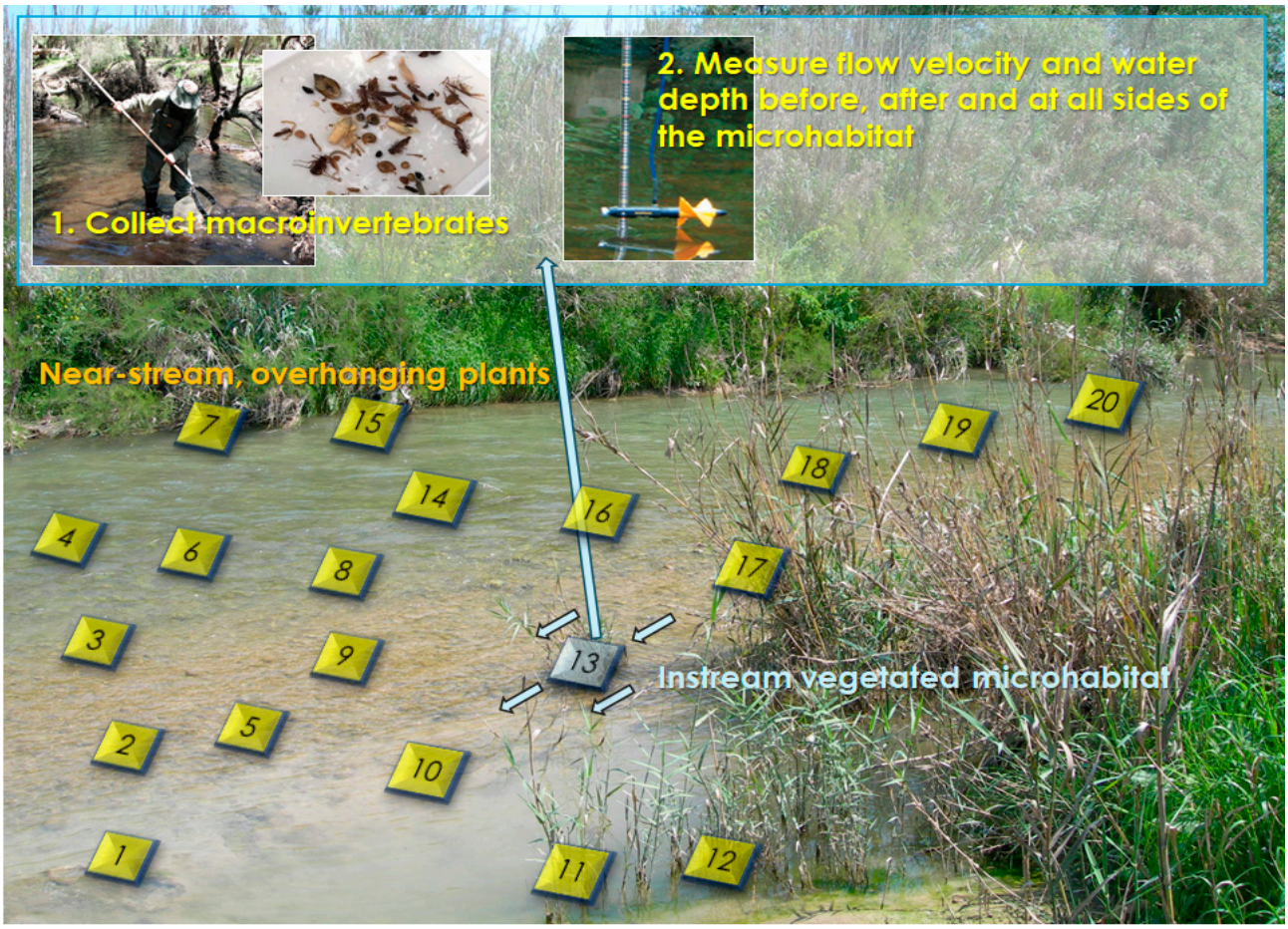

Figure 2. Sampling methodology: a total of 124 microhabitats in the Oinoi Stream and the upper Great Rafina River (Lykorema Stream), Attica, Greece, were sampled for macroinvertebrates, with simultaneous measurements of flow velocity and water depth, before, after, and on each side of each microhabitat.

2.3. Postsampling Analysis

2.3.1. Manning's Roughness Coefficients and Drag Force

Vegetation-adapted Manning's roughness coefficients (n_v) and drag force terms (F_{dx}; F_{dy}; and F_D) were calculated for each vegetation type (excluding algae, free-floating vegetation, and detritus) for three density (d) classes: (1) sparse—$0\% < d \leq 50\%$, (2) moderate—$50\% < d \leq 80\%$, and (3) dense—$80\% < d \leq 100\%$. Manning's n for emergent vegetation (EFL, EBL, and overhanging) was calculated using the following equation by Petryk and Bosmajian [25] for emergent rigid vegetation:

$$n_v = n_o \sqrt{1 + \left(\frac{C_d \sum A_i}{2gAL}\right)\left(\frac{1}{n_o}\right)^2 R^{\frac{4}{3}}} \quad (1)$$

where n_v is the Manning's n for each emergent vegetation type, n_o is the boundary n (the Manning's coefficient for the substrate without vegetation, which was set to 0.03 for clean natural streams based on the previous literature [40]), C_d is the drag coefficient (set to 1 for vegetated channels [41]), A_i is the cross-sectional flow area (m^2), g is the acceleration of gravity (m/s^2), and R is the hydraulic radius (m).

Manning's n for submerged vegetation (SFL, SBL, and bryophytes) was calculated using the following equation by Freeman [42] for flexible submerged vegetation:

$$n_v = K_n 0.183 \left(\frac{E_s A_s}{\rho A_i V_*^2}\right)^{0.183} \left(\frac{H}{Y_o}\right)^{0.243} (MA_i)^{0.273} \left(\frac{\nu}{V_* R}\right)^{0.115} \left(\frac{1}{V_*}\right) R^{\frac{2}{3}} S^{\frac{1}{2}} \quad (2)$$

where n_v is the Manning's n for each submerged vegetation type, K_n is a unit conversion factor (1.0 $m^{1/3}/s$), E_s is the modulus of plant stiffness (Nm^{-2}), A_s is the total area covered by vegetation (m^2), ρ is the fluid density (kg/m^3), A_i is the cross-sectional flow area (m^2), V is the mean flow velocity (m/s), H is the average undeflected plant height (m), Y_o is the water depth (m), M is the relative plant density, V* is the shear velocity (m/s), R is the hydraulic radius, and S is the bed slope.

To facilitate the use of the vegetation-adapted coefficients in ecohydraulic modeling, we further averaged the coefficients of EFL, EBL, and overhanging to derive a single n for emergent vegetation and the coefficients of SFL, SBL, and bryophytes to derive a single n for submerged vegetation.

Additionally, the drag force terms (i.e., F_x and F_y; N/m^2) were estimated according to the work of Sun et al. [15] as follows:

$$F_x = S_x + F_{dx} \Big| F_y = S_y + F_{dy} \quad (3)$$

where S_x and S_y express the bed friction terms derived from the Manning–Strickler formula, while F_{dx} and F_{dy} are the drag force terms resolved in terms of the Chézy's coefficient (x: longitudinal and y: transverse axis). The drag forces (i.e., F_{dx} and F_{dy}; N/m^2) were estimated according to the work of Sun et al. [15] as follows:

$$S_x = -\frac{a}{\cos(\theta)} \frac{gn^2}{h^{\frac{4}{3}}} U\sqrt{U^2+V^2} | S_y = -\frac{a}{\cos(\theta)} \frac{gn^2}{h^{\frac{4}{3}}} V\sqrt{U^2+V^2} \quad (4)$$

$$F_{dx} = -\frac{N}{A}\frac{D}{2} C_d U\sqrt{U^2+V^2} \mid F_{dy} = -\frac{N}{A}\frac{D}{2} C_d V\sqrt{U^2+V^2} \quad (5)$$

where α denotes the vegetation porosity (%), θ is the channel slope, g is the acceleration of gravity (m/s^2), n is Manning's coefficient, h is the water depth between the bottom and the free surface (m), U and V are the longitudinal and lateral velocities (m/s), N is the total vegetation number per area A (m^2), and D is the vegetation diameter (m) [43]. Subsequently, the divergence force (F_D; N/m^2) of the two force components was calculated as:

$$F_D = \sqrt{{F_x}^2 + {F_y}^2} \quad (6)$$

2.3.2. Habitat Suitability

To develop habitat suitability curves (HSCs) for benthic macroinvertebrates, we applied a previously formulated macroinvertebrate-community-based habitat suitability index [2,36] that integrates four metrics that are commonly applied to assess macroinvertebrate habitat suitability [44–47]. These metrics are macroinvertebrate abundance, taxonomic richness, diversity (Shannon's index), and Ephemeroptera–Plecoptera–Trichoptera richness (EPT richness), and they were calculated using the ASTERICS software version 3.1.1 (IRV Software, Vienna, AT, USA). Habitat suitability was calculated as follows:

$$K = 0.4n_m + 0.3H + 0.2EPT + 0.1a \quad (7)$$

where K represents the habitat suitability ranging from 0 (lowest) to 1 (highest), n_m denotes macroinvertebrate taxa richness (No. of families), H is the Shannon's diversity index, EPT is the number of EPT taxa, and a denotes the abundance of benthic macroinvertebrates.

Each microhabitat's K was normalized to a 0–1 scale by dividing by the maximum K value observed at the site of the sampled microhabitat. All K values (for each microhabitat) were further standardized by multiplying by vegetation density, and the overall K for each vegetation type was expressed as the average microhabitat K. An abundance-based habitat suitability was also calculated for each vegetation type and for each macroinvertebrate taxon by summing the abundance of each taxon among the samples of the same vegetation type. Thus, two habitat suitability indices were ultimately developed and applied:

$$K_{VC} = \sum_{i=1}^{N} \frac{K_i d_i}{N} \quad (8)$$

where K_{VC} is the community-based habitat suitability for each vegetation type (ranging from 0 to 1), N is the number of samples of each vegetation type, K_i is the habitat suitability of each sample, and di is the density of the vegetation at each sample (microhabitat) and:

$$K_{Va} = \sum_{1}^{N} a_i \quad (9)$$

where K_{Va} is the taxon-based habitat suitability for each vegetation type (ranging from 0 to 1), N is the number of samples of each vegetation type, and a_i is the abundance of the taxon at each sample.

The calculated habitat suitability for each vegetation type was added to the habitat suitability of the inorganic substrate to which the vegetation was rooted based on a previous habitat suitability assessment for inorganic substrate types [36]. To ensure that no issues of spatiotemporal autocorrelation existed among the samples (for the calculated habitat suitability indices), we applied Moran's autocorrelation coefficient (Moran's I) in R version 4.0.3 [48] using the ape package [49].

3. Results

3.1. Vegetation-Adapted Manning's Roughness Coefficients and Drag Force

In both streams that were examined in this study, the average flow velocity (V) was equal to 0.22 m/s (number of samples (N) = 124; standard error (SE) = ± 0.014; min = 0.033; max = 2.038), and the average water depth was 0.12 m (N = 124; SE = ± 0.004; min = 0.01; max = 0.64). All vegetation types had lower average V downstream of the vegetation patch and higher average V upstream of the vegetation patch (mean difference of 0.093 m/s). The highest V change (Vc) was observed for detritus (N = 23; Vc = −0.18 m/s), and the lowest Vc was observed for overhanging vegetation (N = 16; Vc = −0.03 m/s) (Figure 3). In contrast, the average water depths (D) were similar or slightly higher after the vegetation patches (mean difference of 0.00013 m). The highest D change (Dc) was observed for algae (N = 18; Dc = +0.025 m), and the lowest Dc was observed for emergent broad-leaved vegetation (N = 10; Dc = +0.001 m) (Figure 4).

Manning's n values were higher for all vegetation types compared to n_o, gradually increasing from sparse to dense patches for both emergent and submerged vegetation. Manning's n change (compared to n_o) was +31.70% for emergent vegetation types (N = 34) and +30.32% for submerged vegetation types (N = 45). The highest n change values were observed for dense emergent vegetation (N = 12; n change: 57.07%) and dense submerged vegetation (N = 22; n change = +48.01%). The lowest n change values were observed for sparse submerged vegetation (N = 16; n change = +23.5%) and sparse emergent vegetation (N = 17; n change = +16.49%) (Table 1).

Vegetation-adapted drag force (F_D) was highest in dense vegetation patches, lower in moderate patches, and lowest in sparse vegetation patches for both emergent and submerged vegetation (Table 2). In more detail, F_D was highest in dense SFL (F_D = 0.783; N = 11), followed by dense EFL (F_D = 0.707; N = 6) and dense bryophytes (F_D = 0.592; N = 5), and was lowest in moderate SFL (F_D = 0.016; N = 1), followed by sparse EBL (F_D = 0.141; N = 4) and moderate overhanging vegetation (F_D = 0.252; N = 9).

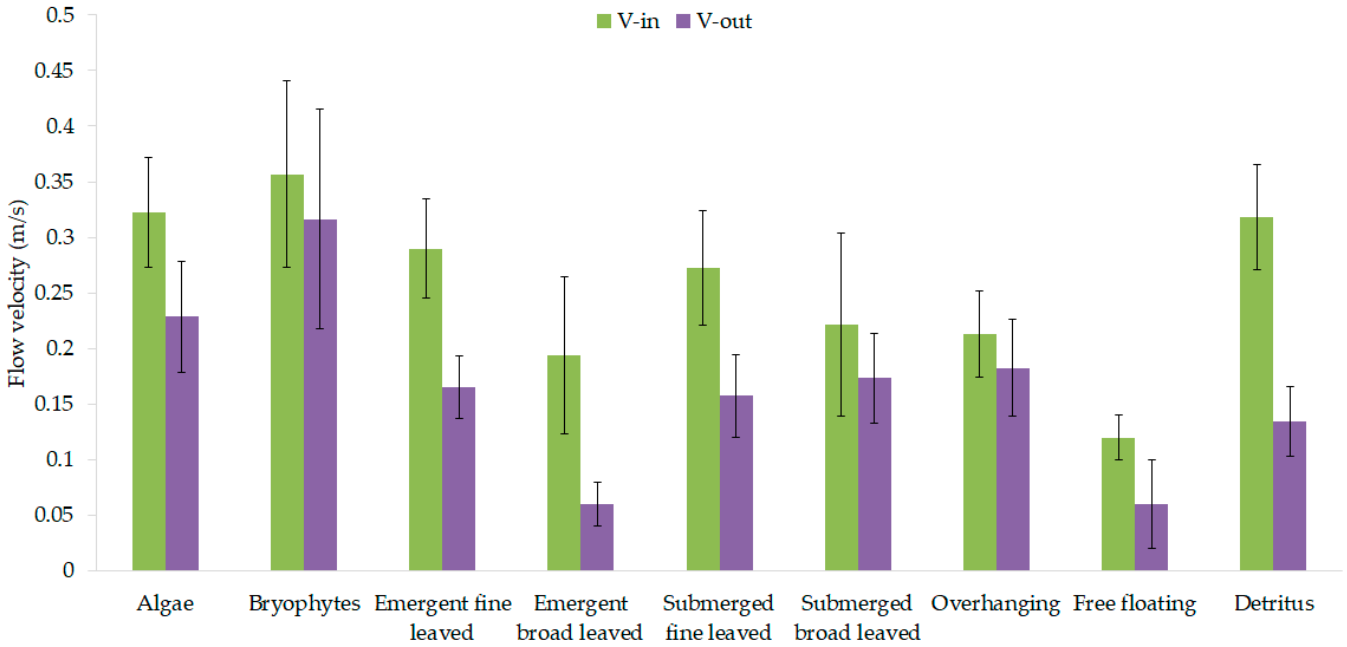

Figure 3. Average (±standard error) flow velocity before (V-in; m/s) and after (V-out; m/s) each vegetation type.

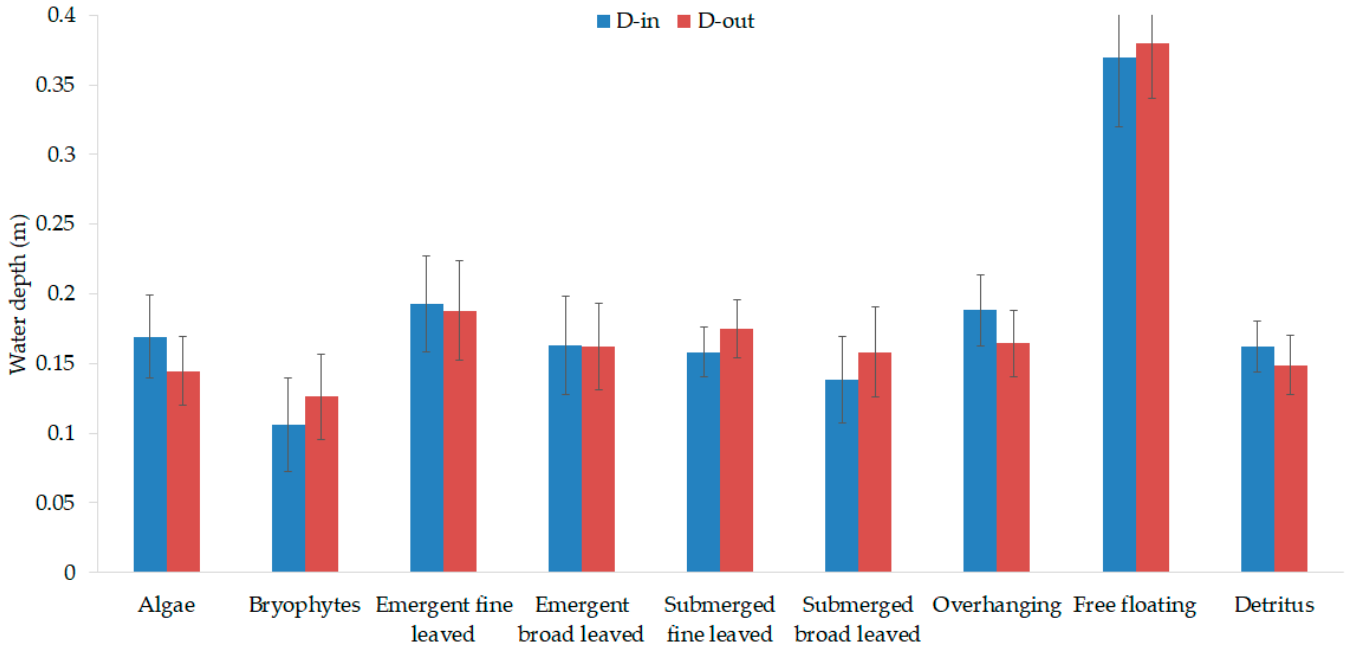

Figure 4. Average (±standard error) water depth before (D-in; m) and after (D-out; m) each vegetation type.

Table 1. Manning's roughness coefficients (n) for emergent and submerged vegetation types in varying densities. Numbers in parentheses indicate the number of samples of each vegetation type.

Vegetation-Adapted Manning's Roughness Coefficients (n)					
	Veg. Type | Veg. Density	**Dense (80% < d ≤ 100%)**	**Moderate (50% < d ≤ 80%)**	**Sparse (0% < d ≤ 50%)**	**Average**
Group 1: Emergent vegetation	Algae	n/a	n/a	n/a	n/a
	Emergent fine-leaved	0.042 (6)	0.042 (6)	0.034 (6)	0.038 (12)
	Emergent broad-leaved	0.052 (1)	0.048 (2)	0.034 (4)	0.039 (6)
	Overhanging	0.047 (5)	0.045 (9)	0.036 (7)	0.041 (16)
	Group 1 average	**0.047 (12)**	**0.045 (17)**	**0.035 (17)**	**0.039 (34)**
Group 2: Submerged vegetation	Submerged fine-leaved	0.052 (7)	0.049 (9)	0.046 (6)	0.048 (15)
	Submerged broad-leaved	0.049 (1)	0.049 (1)	0.038 (4)	0.040 (5)
	Bryophytes	0.032 (5)	0.031 (6)	0.028 (4)	0.029 (10)
	Group 2 average	**0.044 (13)**	**0.043 (16)**	**0.037 (14)**	**0.039 (30)**
	Free-floating	n/a	n/a	n/a	n/a
	Detritus	n/a	n/a	n/a	n/a

Table 2. Drag force (F_D; N/m^2) for emergent and submerged vegetation types in varying densities. Numbers in parentheses indicate the number of samples of each vegetation type.

Vegetation-Adapted Drag Force (F_D)					
	Veg. Type | Veg. Density	**Dense (80% < d ≤ 100%)**	**Moderate (50% < d ≤ 80%)**	**Sparse (0% < d ≤ 50%)**	**Average**
Group 1: Emergent vegetation	Algae	n/a	n/a	n/a	n/a
	Emergent fine-leaved	0.707 (6)	0.707 (6)	0.412 (6)	0.559 (12)
	Emergent broad-leaved	n/a	0.144 (2)	0.141 (4)	0.142 (6)
	Overhanging	0.252 (5)	0.252 (9)	0.352 (7)	0.302 (16)
	Group 1 average	0.478 (11)	0.367 (17)	0.301 (17)	0.334 (34)
Group 2: Submerged vegetation	Submerged fine-leaved	0.783 (7)	0.760 (9)	0.251 (6)	0.505 (15)
	Submerged broad-leaved	0.016 (1)	0.016 (1)	0.045 (4)	0.030 (5)
	Bryophytes	0.592 (5)	0.339 (6)	0.385 (4)	0.029 (10)
	Group 2 average	0.463 (13)	0.371 (16)	0.227 (14)	0.362 (30)
	Free-floating	n/a	n/a	n/a	n/a
	Detritus	n/a	n/a	n/a	n/a

3.2. Macroinvertebrate Habitat Suitability of Various Stream Vegetation Types

In total, 17,248 macroinvertebrate individuals from 72 families were sorted and identified from all stream vegetation types. The taxonomic richness was highest in free-floating vegetation (N = 2; R = 10.2; SE = ± 0.26) and lowest in overhanging vegetation (N = 16; R = 6.44; SE = ± 0.16) (Figure 5). Shannon's diversity varied slightly between vegetation types and was highest in free-floating vegetation (N = 2; H = 1.89; SE = ± 1.76) and lowest in emergent broad-leaved vegetation (N = 10; H = 1.12; SE = ± 0.36). The EPT richness was highest in algae (N = 18; EPT = 3.1; SE = ± 0.06) and submerged fine-leaved vegetation (N = 18; EPT = 3.1; SE = ± 0.11) and lowest in free-floating vegetation (N = 2; EPT = 1.5; SE = ± 0.35).

The macroinvertebrate abundance was highest in free-floating vegetation (N = 2; a = 241.5; SE = ± 20) and lowest in overhanging vegetation (N = 16; a = 28.94; SE = ± 1.6). The macroinvertebrate-community-based habitat suitability was highest for submerged broad-leaved vegetation (N = 6; K = 0.68; SE = ± 0.06) and lowest for bryophytes (N = 13; K = 0.2; SE = ± 0.01) (Figure 6). Emergent and submerged plants had higher habitat suitability compared to nonvascular vegetation (algae and bryophytes) and detritus.

Macroinvertebrate taxa had varying optimal preferences for different vegetation types. The abundance of Athericidae, Hydroptilidae, and Tipulidae was highest in algae, with 42%, 72%, and 50% of individuals, respectively, being found in algae (Figure S1; Supplementary material). The abundance of Elmidae (68%), Empididae (46%), Ephemeridae (100%), Glossiphoniidae

(100%), Lepidostomatidae (92%), Leptoceridae (59%), Leptophlebiidae (100%), Nemouridae (100%), Rhyacophilidae (100%), and Scirtidae (80%) was highest in bryophytes. Calamoceratidae (100%), Dolichopodidae (100%), Dryopidae (57%), Leuctridae (61%), Ostracoda (100%), Physidae (65%), and Polycentropodidae (82%) were more abundant in detritus. The abundance of Calopterygidae (44%), Gyrinidae (80%), Hydrobiidae (68%), Neritidae (70%), and Sphaeriidae (84%) was highest in emergent broad-leaved plants. Ancylidae (60%), Corixidae (86%), Hydrachnidae (60%), and Psychodidae (100%) were more abundant in emergent fine-leaved plants. Hydrometridae (62.5), Libellulidae (43%), and Stratiomyiidae (67%) were more abundant in free-floating plants, and Aeshnidae (55%), Caenidae (53%), and Limoniidae (77%) were more abundant in submerged fine-leaved plants.

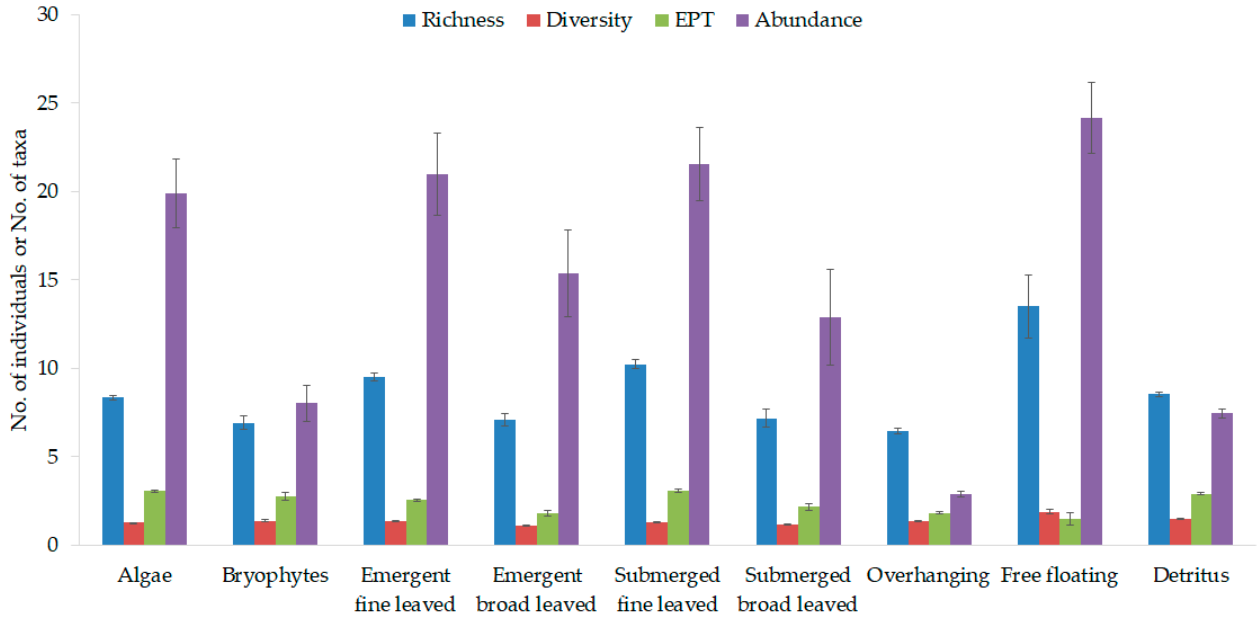

Figure 5. Average (±standard error) taxonomic richness (No. of taxa), Shannon's diversity, Ephemeroptera–Plecoptera–Trichoptera richness (No. of EPT taxa), and total abundance (No. of individuals/10) of benthic macroinvertebrates of each vegetation type.

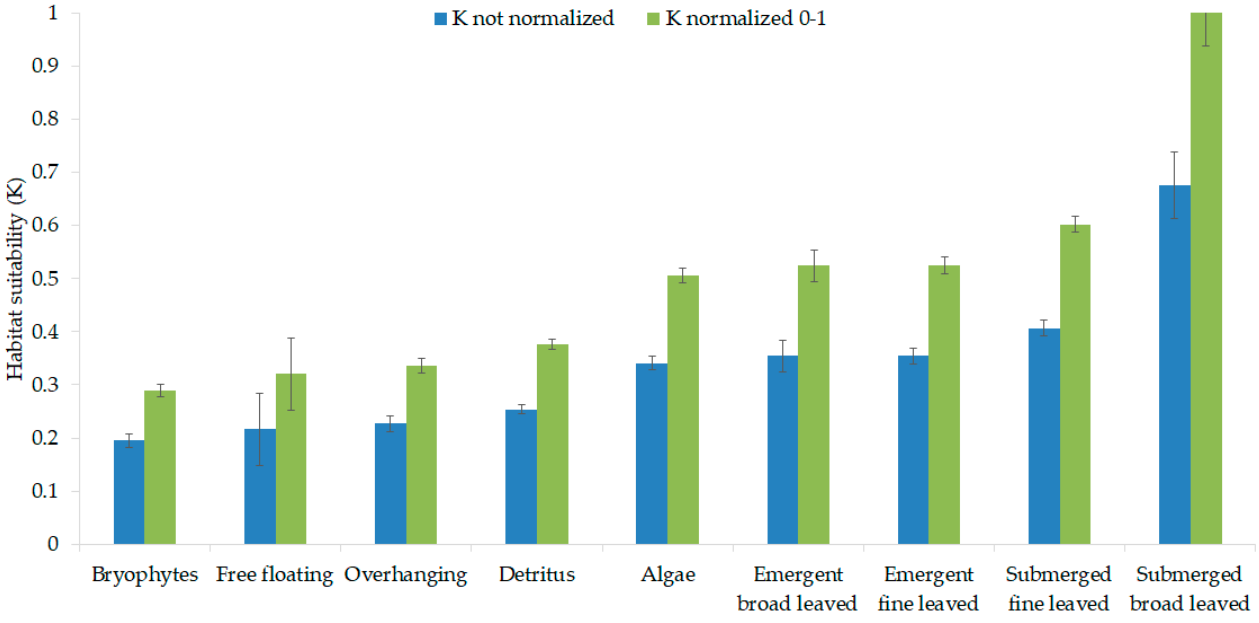

Figure 6. Average (±standard error) macroinvertebrate habitat suitability (K) of each vegetation type.

The habitat suitability values of each vegetation type (added to the inorganic substrate on which the vegetation was rooted) are shown in Table 3. Considering that the habitat suitability was highest in SBL, all SBL added values yielded high suitability, reaching close to 1. Vegetated silt and sand had the lowest values, depending on the vegetation type, but they were highly increased compared to the unvegetated inorganic substrate. The habitat suitability was highest for vegetated small stones, large stones, and boulders.

Table 3. Habitat suitability (0: totally unsuitable; 1: totally suitable) for emergent and submerged vegetation types in combination with the inorganic bottom substrate type. Unvegetated means the habitat suitability of the inorganic substrate type without any vegetation. For each vegetation type, the habitat suitability was added to that of the inorganic substrate, e.g., SFL in silt (0.71) means that the habitat suitability for SFL is 0.71 − 0.30 = 0.41.

Vegetation-Adapted Macroinvertebrate Habit Suitability										
Veg. Type / Substrate	**Unvegetated**	**Algae**	**Bryophytes**	**SFL**	**SBL**	**EFL**	**EBL**	**Overhanging**	**Free-Floating**	**Detritus**
Silt	0.30	0.64	0.50	0.71	0.98	0.65	0.65	0.53	0.52	0.55
Sand	0.45	0.79	0.64	0.85	1.00	0.80	0.80	0.67	0.66	0.70
Fine gravel	0.37	0.71	0.57	0.78	1.00	0.72	0.72	0.60	0.59	0.62
Medium gravel	0.54	0.88	0.74	0.95	1.00	0.90	0.90	0.77	0.76	0.80
Large gravel	0.66	1.00	0.85	1.00	1.00	1.00	1.00	0.88	0.87	0.91
Small stones	0.65	0.99	0.84	1.00	1.00	1.00	1.00	0.88	0.87	0.90
Large stones	0.62	0.96	0.82	1.00	1.00	0.98	0.98	0.85	0.84	0.88
Boulders	0.63	0.97	0.82	1.00	1.00	0.98	0.98	0.86	0.85	0.88

4. Discussion

4.1. Parsimony and the Importance of Including Stream Vegetation in Ecohydraulic Models

A model is a simplification/approximation of a complex reality. Thus, a computer model that will simulate reality in its full complexity is elusive [50]. This is also the case for hydroecological models; these models can be useful when they include as many physical-hydrological-hydraulic variables as necessary to explain ecological processes, but they may become practically useless when more and more variables are included, especially when their explanatory power is low. Consequently, the challenge in hydroecological modeling is to formulate a parsimonious model that will accurately approximate reality with as few predictor variables as possible [51]. For ecohydraulic models, these 'few predictors' that primarily determine the distribution of freshwater biota had long been (i) flow velocity, (ii) water depth (both reflecting the microhabitat effect of water discharge fluctuations), and (iii) the type of substrate (boulders, pebbles, cobbles, etc.) [2,35,52]. Are these three variables enough to assume a parsimonious ecohydraulic model?

Previous research suggests that two more physical variables are major determinants of hydroecological processes in freshwaters: stream vegetation and water temperature. In this study, we focused on stream vegetation, the presence of which modifies flow and sediment transport patterns [12,16] and increases habitat and biological diversity [14,15]. Thus, V-D-S-based ecohydraulic models (i3 models) may oversimplify hydroecological processes; we argue that they are useful as a start and can indeed provide confident predictions [36] but should be enhanced to include stream vegetation and water temperature (i5 models) to increase their accuracy and optimally approximate hydroecological reality in a way that can be characterized as parsimonious. While the data to develop i3 ecohydraulic models are becoming more and more available worldwide, in this study we further collected the field data necessary (hydraulic and habitat) to enable advancing to i4 ecohydraulic models (including vegetation) and further on, when water temperature data become widely available, to i5 ecohydraulic models.

4.2. How to Include Stream Vegetation in the Hydraulic Module

What mostly matters in the hydraulic modules of ecohydraulic models is to accurately and cost-effectively calibrate and validate them [53,54]. At least two sets of V and D field observations (i.e., in two different discharges) are required, one for calibration and one for validation. Calibration is commonly applied by adjusting the Manning's n values across the

river reach (in different sections) until, for the first discharge dataset, there is a match (often > 90% is required) between the simulated and observed V and D values [55]. Then, the calibrated model is used to simulate V and D values for the second discharge dataset (no further n adjustment is applied), and the model is considered validated if there is another a > 90% match between the simulated and observed V and D data. In vegetated streams, this process may become very challenging, especially if the user starts calibrating with arbitrary n values. We suggest that prior to calibrating/validating a vegetation-including model the user should have at least a rough estimation of the vegetation distribution across the stream reach (either using photographic material or satellite imagery). Then, the user could apply our vegetation-adapted n values (n_v) to start calibrating. It is possible that the additive approach of Cowan [56] should be applied. In this approach, the n that should be used is the adjusted sum of several coefficients [18,21], as follows:

$$n = (n_o + n_1 + n_2 + n_3 + n_4)m_5 \quad (10)$$

where n_o is a basic n value for a straight, uniform, smooth channel; n_1 is the adjustment factor for the effect of surface irregularity; n_2 is the adjustment factor for the effect of variation in the shape and size of the channel cross-section; n_3 is the adjustment factor for obstruction; n_4 is the adjustment factor for vegetation (our n_v); and m_5 is a correction factor for meandering channels. For example, in the case of emergent broad-leaved plants rooted in boulders, the user would likely add $n_o = 0.07 + n_4 = 0.039 \Leftrightarrow n \approx 0.11$ or even apply the m_5 factor if there such information was available.

4.3. How to Include Stream Vegetation in the Habitat Module

Stream vegetation (B) in habitat modules/models can be included by expanding the two options for using habitat suitability: habitat suitability curves (HSCs) and fuzzy habitat suitability rules (HSRs). Within the HSC approach, at each node of the computational mesh representing the stream reach, V-suitability is often multiplied by D-suitability and S-suitability to calculate the overall node-specific suitability (or a geometric mean is often calculated). Macroinvertebrate B-suitability (based on Table 3) can thus be included by multiplying the V-, D-, and S-suitabilities with the B-suitability or by calculating a geometric mean of the four variables. If the HSR approach is to be applied, an advanced fuzzy rule-based algorithm should be formulated, which also includes vegetation-specific habitat suitability rules. For example, IF V is moderate AND D is shallow AND S is boulders AND B is EBL THEN habitat suitability is high (and so on) [36,57].

4.4. i5 Ecohydraulics: Implications and Future Research

Typically, stream vegetation has been introduced in (eco)hydraulic models by appropriately modifying various bed roughness coefficients [58]. These roughness coefficients have commonly been calculated based on equations including flow velocity, water depth, the type of substrate, and the density of the vegetation patch [40,59–61]. Morphological features of stream vegetation were further included in more advanced equations [28,42]. Our results showed that the effect of stream vegetation on Manning's n was type-dependent (varying between emergent rigid and submerged flexible vegetation) and increased by increasing the vegetation density. Consequently, future studies may focus on this morphological variability of stream vegetation, potentially developing indices, such as the leaf area index [30], that would more accurately introduce the morphological variability of stream vegetation into ecohydraulic models.

As discussed earlier, i4 models (those that simulate the hydroecological effects of stream vegetation) may be considered an intermediate step to ultimately advance to the optimal (parsimonious) i5 ecohydraulic models (those that further simulate the hydroecological effects of water temperature), considering that all five physical/hydraulic variables are critical determinants of the distribution of freshwater biota. However, i5 models may require increased computational power, especially their habitat modules. The HSC approach is less demanding; stream vegetation only needs to be included in the equation that

computes the overall habitat suitability (either a product or a geometric mean of V, D, S, and B habitat suitability). The HSRs approach, which takes into account the interactions between V, D, S, and B is closer to how natural/ecological processes operate and may dramatically increase computational times. For example, an HSR-based model including five V classes, five D classes, eight S classes, and our nine-class stream vegetation would require 1800 rules to operate. If another five classes of water temperature are included, the number becomes 9000 rules that need to be checked at each node. Still, the rapid increase in computational power will probably soon tackle this issue. We suggest that future research should focus on collecting field hydroecological data (i) from stream/river reaches around the world to compare and enable the application of localized i4 ecohydraulic models and (ii) on the influence of water temperature on freshwater biota that could be used in i5 ecohydraulic models.

5. Conclusions

Current ecohydraulic applications commonly use three predictor variables (i3 models) to simulate the habitat suitability of aquatic biota in various discharges. These i3 models have often resulted in accurate simulations, mostly depending on the purpose of each application, but they may also oversimplify the hydroecological reality (in real life, aquatic biota respond to a multitude of interacting environmental variables). In this study, we argue that i3 models should not be considered parsimonious and suggest that ecohydraulic research should focus on developing advanced ecohydraulic models (both conceptual models and the relevant computer software) that will include two additional predictors: stream vegetation (i4 models) and water temperature (i5 models).

We acknowledge, however, that the frequent lack of field data may inhibit such efforts towards i5 ecohydraulics. To this end, we hereby provide field-calculated Manning's roughness coefficients for nine types of submerged, emergent, and overhanging stream vegetation, together with guidance on how to include these data in the hydraulic and habitat modules of i4 ecohydraulic models. Although locally restricted, the data of this study may be appropriately calibrated/adjusted for use in ecohydraulic applications in river reaches with similar hydroecological properties. We further argue that parsimony in ecohydraulic models should be sought in i5 models and suggest that future research should focus on collecting the data necessary to develop such models.

Supplementary Materials: The following supporting information can be downloaded at: https://www.mdpi.com/article/10.3390/w14223727/s1, Figure S1: Abundance-based habitat suitability (average: total abundance divided by the number of sampled microhabitats) of each type of bottom/riparian vegetation for each macroinvertebrate taxon.

Author Contributions: Conceptualization, C.T. and A.S.; methodology, C.T.; formal analysis, C.T., G.V. and I.K.; resources, A.S.; data curation, C.T., G.V., I.K. and K.G.; writing—original draft preparation, C.T. and G.V.; writing—review and editing, C.T., A.S., K.G. and I.K.; visualization, C.T.; supervision, K.G. and A.S.; project administration, A.S.; funding acquisition, C.T. and A.S. All authors have read and agreed to the published version of the manuscript.

Funding: This research was funded by the Basic Research Programme Committee (PEVE 2020) of the National Technical University of Athens, Greece, SARF No. 65228200.

Data Availability Statement: The data of this study are available from the authors upon relevant request.

Conflicts of Interest: The authors declare no conflict of interest.

References

1. Harlow, F.H. Fluid dynamics in Group T-3 Los Alamos National Laboratory (LA-UR-03-3852). *J. Comput. Phys.* **2004**, *195*, 414–433. [CrossRef]
2. Theodoropoulos, C.; Skoulikidis, N.; Rutschmann, P.; Stamou, A. Ecosystem-based environmental flow assessment in a Greek regulated river with the use of 2D hydrodynamic habitat modelling. *River Res. Appl.* **2018**, *34*, 538–547. [CrossRef]

3. Stuart, I.G.; Sharpe, C.P. Ecohydraulic model for designing environmental flows supports recovery of imperiled Murray cod (*Maccullochella peelii*) in the Lower Darling–Baaka River following catastrophic fish kills. *Mar. Freshw. Res.* **2021**, *73*, 247–258. [CrossRef]
4. Hardy, T.; Kollaus, K.; Tolman, K.; Heard, T.; Howard, M. Ecohydraulics in applied river restoration: A case study in the San Marcos River, Texas, USA. *J. Appl. Water Eng. Res.* **2016**, *4*, 2–10. [CrossRef]
5. Theodoropoulos, C.; Stamou, A.; Vardakas, L.; Papadaki, C.; Dimitriou, E.; Skoulikidis, N.; Kalogianni, E. River restoration is prone to failure unless pre-optimized within a mechanistic ecological framework | Insights from a model-based case study. *Water Res.* **2020**, *173*, 115550. [CrossRef] [PubMed]
6. Vowles, A.; Eakins, L.R.; Piper, A.T.; Kerr, J.; Kemp, P.S. Developing realistic fish passage criteria: An ecohydraulics approach. In *Ecohydraulics: An Integrated Approach*; Maddock, I., Harby, A., Kemp, P., Wood, P.J., Eds.; Wiley-Blackwell: Chichester, UK, 2013; pp. 143–156.
7. Mitsopoulos, G.; Theodoropoulos, C.; Papadaki, C.; Dimitriou, E.; Santos, J.M.; Zogaris, S.; Stamou, A. Model-based ecological optimization of vertical slot fishways using macroinvertebrates and multispecies fish indicators. *Ecol. Eng.* **2020**, *158*, 106081. [CrossRef]
8. Maddock, I.; Harby, A.; Kemp, P.; Wood, P.J. *Ecohydraulics: An Integrated Approach*; Wiley and Sons: Chichester, UK, 2013.
9. Zeiringer, B.; Seliger, C.; Greimel, F.; Schmutz, S. River hydrology, flow alteration, and environmental flow. In *Riverine Ecosystem Management*; Schmutz, S., Sendzimir, J., Eds.; Springer: Berlin/Heidelberg, Germany, 2018; pp. 67–89.
10. Acreman, M.C.; Dunbar, M.J. Defining environmental river flow requirements: A review. *Hydrol. Earth Syst. Sci.* **2004**, *8*, 861–876. [CrossRef]
11. Gopal, B. Methodologies for the assessment of environmental flows. In *Environmental Flows: An Introduction for Water Resources Managers*; Gopal, B., Ed.; National Institute of Ecology: New Delhi, India, 2012.
12. Vargas-Luna, A.; Crosato, A.; Uijttewaal, W.S.J. Effects of vegetation on flow and sediment transport: Comparative analyses and validation of predicting models. *Earth Surf. Process. Landf.* **2015**, *40*, 157–176. [CrossRef]
13. Huttunen, K.L.; Mykrä, H.; Oksanen, J.; Astorga, A.; Paavola, R.; Muotka, T. Habitat connectivity and in-stream vegetation control temporal variability of benthic invertebrate communities. *Sci. Rep.* **2017**, *7*, 1448. [CrossRef]
14. Tessier, C.; Cattaneo, A.; Pinel-Alloul, B.; Galanti, G.; Morabito, G. Biomass, composition and size structure of invertebrate communities associated to different types of aquatic vegetation during summer in Lago di Candia (Italy). *J. Limnol.* **2004**, *63*, 190–198. [CrossRef]
15. Sun, X.; Shiono, K.; Rameshwaran, P.; Chandler, J.H. Modelling vegetation effects in irregular meandering river. *J. Hydraul. Res.* **2010**, *48*, 775–783. [CrossRef]
16. Benifei, R.; Solari, L.; Vargas-Luna, A.; Geerling, G.; Van Oorschot, M. Effect of vegetation on floods: The case of river Magra. In Proceedings of the 36th IAHR World Congress, The Hague, The Netherlands, 28 June–3 July 2015.
17. Theodoropoulos, C.; Syrmou, E.; Karaouzas, I.; Gritzalis, K.; Stamou, A. Simulated effects of streambed vegetation on river hydraulics and the habitat suitability of freshwater macroinvertebrates. In Proceedings of the 17th International Conference on Environmental Science and Technology, Athens, Greece, 1–4 September 2021.
18. Lama, G.F.C.; Errico, A.; Francalanci, S.; Solari, L.; Chirico, G.B.; Preti, F. Hydraulic modeling of field experiments in a drainage channel under different riparian vegetation scenarios. In *Innovative Biosystems Engineering for Sustainable Agriculture, Forestry and Food Production*; Coppola, A., Di Renzo, G., Altieri, G., D'Antonio, P., Eds.; Springer: Cham, Switzerland, 2020; pp. 69–77.
19. Lama, G.F.C.; Crimaldi, M.; Pasquino, V.; Padulano, R.; Chirico, G.B. Bulk drag predictions of riparian *Arundo donax* stands through UAV-acquired multispectral images. *Water* **2021**, *13*, 1333. [CrossRef]
20. Lama, G.F.C.; Errico, A.; Pasquino, V.; Mirzaei, S.; Preti, F.; Chirico, G.B. Velocity uncertainty quantification based on riparian vegetation indices in open channels colonized by *Phragmites australis*. *J. Ecohydraulics* **2022**, *7*, 71–76. [CrossRef]
21. Errico, A.; Lama, G.F.C.; Francalanci, S.; Chirico, G.B.; Solari, L.; Preti, F. Flow dynamics and turbulence patterns in a drainage channel colonized by common reed (*Phragmites australis*) under different scenarios of vegetation management. *Ecol. Eng.* **2019**, *133*, 39–52. [CrossRef]
22. Xu, W.; Zhang, H.; Jing, Y.; Wang, Z.; Ji, C.; Zhang, H. A study on Manning's coefficient of rigid unsubmerged vegetation under open channel constant gradual flow condition. In Proceedings of the ASME 2010 International Mechanical Engineering Congress and Exposition, ASMEDC, Vancouver, BC, Canada, 12–18 November 2010.
23. Fathi-Moghadam, M.; Kashefipour, M.; Ebrahimi, N.; Emamgholizadeh, S. Physical and numerical modeling of submerged vegetation roughness in rivers and flood plains. *J. Hydrol. Eng.* **2011**, *16*, 858–864. [CrossRef]
24. Aberle, J.; Järvelä, J. Flow resistance of emergent rigid and flexible floodplain vegetation. *J. Hydraul. Res.* **2013**, *51*, 33–45. [CrossRef]
25. Petryk, S.; Bosmajian, G. Analysis of flow through vegetation. *J. Hydraul. Div.* **1975**, *101*, 871–884. [CrossRef]
26. Cantisani, A.; Giosa, L.; Mancusi, L.; Sole, A. FLORA-2D: A new model to simulate the inundation in areas covered by flexible and rigid vegetation. *Int. J. Eng. Innov. Technol.* **2014**, *3*, 179–186.
27. Shields, F.D.; Coulton, K.G.; Nepf, H. Representation of Vegetation in Two-Dimensional Hydrodynamic Models. *J. Hydraul. Eng.* **2017**, *143*, 02517002. [CrossRef]
28. Lama, G.F.C.; Errico, A.; Francalanci, S.; Solari, L.; Preti, F.; Chirico, G.B. Evaluation of flow resistance models based on field experiments in a partly vegetated reclamation channel. *Geosciences* **2020**, *10*, 47. [CrossRef]

29. Lama, G.F.C.; Giovannini, R.M.; Errico, A.; Mirzaei, S.; Padulano, R.; Chirico, G.B.; Preti, F. Hydraulic efficiency of green-blue flood control scenarios for vegetated rivers: 1D and 2D unsteady simulations. *Water* **2021**, *13*, 2620. [CrossRef]
30. Box, W.; Järvelä, J.; Västilä, K. Flow resistance of floodplain vegetation mixtures for modelling river flows. *J. Hydrol.* **2021**, *601*, 110467. [CrossRef]
31. Lama, G.F.C.; Sadeghifar, T.; Azad, M.T.; Sihag, P.; Kisi, O. On the indirect estimation of wind wave heights over the southern coasts of Caspian Sea: A comparative analysis. *Water* **2022**, *4*, 843. [CrossRef]
32. Sadeghifar, T.; Lama, G.F.C.; Sihag, P.; Bayram, A.; Kisi, O. Wave height predictions in complex sea flows through soft computing models: Case study of Persian Gulf. *Ocean. Eng.* **2022**, *245*, 110467. [CrossRef]
33. Marjoribanks, T.I.; Hard, R.J.; Lane, S.N.; Tancock, M.J. Patch-scale representation of vegetation within hydraulic models. *Earth Surf. Process. Landf.* **2017**, *42*, 699–710. [CrossRef]
34. Bovee, K.D. *Development and Evaluation of Habitat Suitability Criteria for Use in the Instream Flow Incremental Methodology*; Instream Flow Information Paper #21 FWS/OBS-86/7; USDI Fish and Wildlife Service: Washington, DC, USA, 1986.
35. Muñoz-Mas, R.; Martínez-Capel, F.; Schneider, M.; Mouton, A.N. Assessment of brown trout habitat suitability in the Jucar River Basin (SPAIN): Comparison of data-driven approaches with fuzzy-logic models and univariate suitability curves. *Sci. Total Environ.* **2012**, *440*, 123–131. [CrossRef]
36. Theodoropoulos, C.; Vourka, A.; Skoulikidis, N.; Rutschmann, P.; Stamou, A. Evaluating the performance of habitat models for predicting the environmental flow requirements of benthic macroinvertebrates. *J. Ecohydraulics* **2018**, *3*, 30–44. [CrossRef]
37. Campaioli, S.; Ghetti, P.F.; Minelli, A. Manuale per il Riconoscimento dei Macroinvertebrati Delle Acque Dolci Italiane. Provincia Autonoma di Trento: Trento, Italy, 1994.
38. Tachet, H.; Richoux, P.; Bournaud, M.; Usseglio-Polatera, P. *Invertebres d'eau Douche: Systematique, Biologie, Ecologie*; CNRS: Paris, France, 2010.
39. Patsia, A.; Lazaridou, M. *Water Quality through the Directive 2000/60 E.C.: Guide for Benthic Invertebrates of Running Waters of Greece*; ION: Athens, Greece, 2011.
40. Chow, V.T. *Open Channel Hydraulics*; McGraw-Hill: New York, NY, USA, 1959.
41. Stamou, A.; Papadonikolaki, G.; Gkesouli, A. Modeling the flow in an experimental flume with submerged rigid elements. In Proceedings of the 2nd IAHR Europe Congress, Munich, Germany, 27–29 June 2012.
42. Freeman, G.E.; Rahmeyer, W.; Copeland, R.R. *Determination of Resistance Due to Shrubs and Woody Vegetation*; ERDC/CHL TR-00-25, U.S. Army Engineer; Coastal and hydraulics Laboratory: Vicksburg, MS, USA, 2000.
43. Hervouet, J.M. *Hydrodynamics of Free Surface Flows: Modelling with the Finite Element Method*; John Wiley & Sons Ltd.: Chichester, UK, 2007.
44. Englund, G.; Malmqvist, B. Effects of flow regulation, habitat area and isolation on the macroinvertebrate fauna of rapids in North Swedish Rivers. *Regul. Rivers Res. Manag.* **1996**, *12*, 433–445. [CrossRef]
45. Monk, W.A.; Wood, P.J.; Hannah, D.M.; Wilson, D.A.; Extence, C.A.; Chadd, R.P. Flow variability and macroinvertebrate community response within riverine systems. *River Res. Appl.* **2006**, *22*, 595–615. [CrossRef]
46. Waddle, T.J.; Holmquist, J.G. Macroinvertebrate response to flow changes in a subalpine stream: Predictions from two-dimensional hydrodynamic models. *River Res. Appl.* **2011**, *29*, 366–379. [CrossRef]
47. Holmquist, J.G.; Schmidt-Gengenbach, J.; Roche, J.W. Stream macroinvertebrates and habitat below and above two wilderness fords used by mules, horses, and hikers in Yosemite National Park. *W. N. Am. Nat.* **2015**, *75*, 311–324. [CrossRef]
48. R Core Team. *R: A Language and Environment for Statistical Computing*; R Foundation for Statistical Computing: Vienna, Austria, 2022.
49. Paradis, E.; Blomberg, S.; Bolker, B.; Brown, J.; Claramunt, S.; Claude, J.; Cuong, H.S.; Desper, R.; Didier, G.; Durand, B.; et al. *Ape: Analyses of Phylogenetics and Evolution. R package v5.6-2*. Available online: https://cran.r-project.org/web/packages/ape/index.html (accessed on 11 October 2022).
50. de Leeuw, J. Model selection in multinomial experiments. In *On Model Uncertainty and Its Statistical Implications. Lecture Notes in Economics and Mathematical Systems*; Dijkstra, T.K., Ed.; Springer Verlag: New York, NY, USA, 1988; pp. 118–138.
51. Koutsoyiannis, D. Seeking parsimony in hydrology and water resources technology. European Geosciences Union General Assembly, Vienna, Austria. *Geophys. Res. Abstr.* **2009**, *11*, 11469.
52. Dunbar, M.J.; Pedersen, M.L.; Cadman, D.; Extence, C.; Waddingham, J.; Chadd, R.; Larsen, S.E. River discharge and local-scale physical habitat influence macroinvertebrate LIFE scores. *Freshw. Biol.* **2010**, *55*, 226–242. [CrossRef]
53. Liu, J.; Jiang, L.; Bandini, F.; Kittel, C.M.M.; Balbarini, N.; Hansted, N.G.; Grosen, H.; Bauer-Gottwein, P. Spatio-temporally varying Strickler coefficient: A calibration approach applied to a Danish river using in-situ water surface elevation and UAS altimetry. *J. Hydrol.* **2022**, *613*, 128443. [CrossRef]
54. Kittel, C.M.M.; Hatchard, S.; Neal, J.C.; Nielsen, K.; Bates, P.D.; Bauer-Gottwein, P. Hydraulic model calibration using CryoSat-2 observations in the Zambezi catchment. *Water Resour. Res.* **2021**, *57*, e2020WR029261. [CrossRef]
55. Theodoropoulos, C.; Georgalas, S.; Mamassis, N.; Stamou, A.; Skoulikidis, N. Comparing environmental flow scenarios from hydrological methods, legislation guidelines and hydrodynamic habitat models downstream of the Marathon Dam (Attica, Greece). *Ecohydrology* **2018**, *11*, e2019. [CrossRef]
56. Cowan, W.L. Estimating hydraulic roughness coefficients. *Agric. Eng.* **1956**, *37*, 473–475.
57. Theodoropoulos, C.; Skoulikidis, N.; Stamou, A. Habfuzz: A tool to calculate the instream hydraulic habitat suitability using fuzzy logic and fuzzy Bayesian inference. *J. Open Source Softw.* **2016**, *1*, 82. [CrossRef]

58. Díaz, R.G. Analysis of Manning coefficient for small-depth flows on vegetated beds. *Hydrol. Process.* **2005**, *19*, 3221–3233. [CrossRef]
59. Ree, W.O.; Palmer, V.J. *Flow of Water in Channels Protected by Vegetative Linings*; Technical Bulletin; US Soil Conservation Service: Washington DC, USA, 1949; p. 119.
60. Einstein, H.A.; Banks, R.B. Fluid resistance of composite roughness. *Eos Trans. Am. Geophys. Union* **1950**, *31*, 603–610. [CrossRef]
61. Sayer, W.W. Roughness spacing in rigid open channels. *J. Hydraul. Div.* **1961**, *87*, 121–150. [CrossRef]